

University of Nebraska - Lincoln
DigitalCommons@University of Nebraska - Lincoln

USGS Staff -- Published Research

US Geological Survey

2016

Deep subsurface drip irrigation using coal-bed sodic water: Part II. Geochemistry

Carleton R. Bern

Denver Federal Center, cbern@usgs.gov

George N. Breit

Denver Federal Center


Richard W. Healy

Denver Federal Center

John W. Zupancic

BeneTerra LLC, 1415 N. Main St., Sheridan, WY

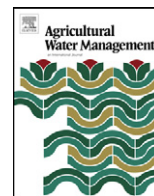
Follow this and additional works at: <http://digitalcommons.unl.edu/usgsstaffpub>

 Part of the [Geology Commons](#), [Oceanography and Atmospheric Sciences and Meteorology Commons](#), [Other Earth Sciences Commons](#), and the [Other Environmental Sciences Commons](#)

Bern, Carleton R.; Breit, George N.; Healy, Richard W.; and Zupancic, John W., "Deep subsurface drip irrigation using coal-bed sodic water: Part II. Geochemistry" (2016). *USGS Staff -- Published Research*. 912.

<http://digitalcommons.unl.edu/usgsstaffpub/912>

This Article is brought to you for free and open access by the US Geological Survey at DigitalCommons@University of Nebraska - Lincoln. It has been accepted for inclusion in USGS Staff -- Published Research by an authorized administrator of DigitalCommons@University of Nebraska - Lincoln.



Deep subsurface drip irrigation using coal-bed sodic water: Part II. Geochemistry

Carleton R. Bern^{a,*}, George N. Breit^a, Richard W. Healy^b, John W. Zupancic^c

^a *Crustal Geophysics and Geochemistry Science Center, U.S. Geological Survey, Denver Federal Center, Denver, CO 80225, USA*

^b *National Research Program, U.S. Geological Survey, Denver Federal Center, Denver, CO 80225, USA*

^c *BeneTerra LLC, 1415 N. Main St., Sheridan, WY 82801, USA*

ARTICLE INFO

Article history:

Received 14 March 2012

Accepted 16 November 2012

Available online 25 December 2012

Keywords:

Gypsum

PHREEQC

Powder River Basin, Wyoming

Sodium adsorption ratio

Sulfuric acid

ABSTRACT

Waters with low salinity and high sodium adsorption ratios (SARs) present a challenge to irrigation because they degrade soil structure and infiltration capacity. In the Powder River Basin of Wyoming, such low salinity (electrical conductivity, EC 2.1 mS cm⁻¹) and high-SAR (54) waters are co-produced with coal-bed methane and some are used for subsurface drip irrigation (SDI). The SDI system studied mixes sulfuric acid with irrigation water and applies water year-round via drip tubing buried 92 cm deep. After six years of irrigation, SAR values between 0 and 30 cm depth (0.5–1.2) are only slightly increased over non-irrigated soils (0.1–0.5). Only 8–15% of added Na has accumulated above the drip tubing. Sodicity has increased in soil surrounding the drip tubing, and geochemical simulations show that two pathways can generate sodic conditions. In soil between 45-cm depth and the drip tubing, Na from the irrigation water accumulates as evapotranspiration concentrates solutes. SAR values >12, measured by 1:1 water–soil extracts, are caused by concentration of solutes by factors up to 13. Low-EC (<0.7 mS cm⁻¹) is caused by rain and snowmelt flushing the soil and displacing ions in soil solution. Soil below the drip tubing experiences lower solute concentration factors (1–1.65) due to excess irrigation water and also contains relatively abundant native gypsum (2.4 ± 1.7 wt.%). Geochemical simulations show gypsum dissolution decreases soil–water SAR to <7 and increases the EC to around 4.1 mS cm⁻¹, thus limiting negative impacts from sodicity. With sustained irrigation, however, downward flow of excess irrigation water depletes gypsum, increasing soil–water SAR to >14 and decreasing EC in soil water to 3.2 mS cm⁻¹. Increased sodicity in the subsurface, rather than the surface, indicates that deep SDI can be a viable means of irrigating with sodic waters.

Published by Elsevier B.V.

1. Introduction

An irrigation method has been developed to dispose of a portion of the large volumes of sodic waters co-produced by coal-bed methane energy (CBM) development in the semi-arid Powder River Basin, while also putting the waters to beneficial use (Zupancic et al., 2008). The method combines year-round irrigation, acidification of the CBM water by addition of sulfuric acid (H₂SO₄), and deep placement of drip tubing for subsurface drip irrigation (SDI). Year-round irrigation is required to keep pace with water production from gas wells. As will be shown here, acidification helps to mitigate the impact of the sodic waters on soil. Deep placement (92 cm) of the drip tubing prevents frost damage to the system during winter operation and helps prevent Na from the irrigation water from rising to the soil surface. Between 2000 and 2010, over 9.8 × 10⁸ m³ of CBM water were produced in the Wyoming portion of Powder River Basin (Wyoming Oil and Gas Conservation Commission,

2011). Currently, SDI systems like the one described utilize about 5% of annual CBM water production in the Powder River Basin (Don Fischer, Wyoming Department of Environmental Quality, personal communication, 3/3/2011).

The CBM water in the Powder River Basin is attractive to agriculture because some of it is low-salinity (ranges: EC = 0.3–4.1 mS cm⁻¹, total dissolved solids, TDS = 200–4000 mg L⁻¹) (Bartos and Ogle, 2002; Jackson and Reddy, 2007; Rice et al., 2002). In contrast, waters co-produced from traditional oil and gas wells are much more saline (Wyoming median TDS = 6500 mg L⁻¹) (Breit, 2011). Sulfate reduction, cation exchange, microbial processes and precipitation of carbonate minerals in the source rocks cause groundwater in the methane-producing coal beds to evolve to a characteristic Na–HCO₃ composition (Brinck et al., 2008; Van Voast, 2003). The sodium adsorption ratio (SAR) is a common measure of sodicity and is calculated as

$$\text{SAR} = \frac{[\text{Na}^+]}{([\text{Ca}^{2+}] + [\text{Mg}^{2+}])^{1/2}} \quad (1)$$

* Corresponding author. Tel.: +1 303 236 1024; fax: +1 303 236 3200.
E-mail address: cbern@usgs.gov (C.R. Bern).

where concentrations are millimoles per liter. Units of SAR are $\text{mmol}^{1/2} \text{L}^{-1/2}$, but common convention is to omit units in reporting the values. Surveys of water compositions from CBM wells in the Powder River Basin found SAR values ranging from 5 to 69 (Bartos and Ogle, 2002; Jackson and Reddy, 2007; Rice et al., 2002). Such SAR values indicate that some CBM waters in the Powder River Basin pose no hazard to soil if used for irrigation, while others pose a severe hazard to soil structure (Ayers and Westcot, 1985). Increasing the proportion of Na^+ on the exchange sites of expansive clays results in greater hydration (swelling) which disrupts soil structure through disaggregation and dispersion of clays (Quirk, 1986). The swelling is increased with greater activity of water (lower salinity), as well as higher pH which favors repulsion of clay particles (Rengasamy and Sumner, 1998). Soils exhibiting physical effects from high sodicity and low salinity can suffer from crusting, erosion, poor aeration and lack of infiltration (Oster and Jayawardne, 1998). Bicarbonate alkalinity poses an additional problem for irrigation, as has been seen in other settings (Bajwa et al., 1992). Upon contact with soil, the bicarbonate (HCO_3^-) can combine with available soil solution Ca^{2+} to precipitate as calcite (CaCO_3), driving EC lower and SAR higher.

Surface irrigation with CBM water in the Powder River Basin increases the SAR and EC of saturated paste extracts and causes Na to accumulate in soils (Ganjegunte et al., 2005). While irrigation can increase biomass in the short-term, over time it can result in accumulation of salts and degradation of soil structure (Ganjegunte et al., 2008; Vance et al., 2008). Even a single year of sodic-water irrigation can be sufficient to decrease infiltration rates (Johnston et al., 2011). A study tested Powder River Basin soils under cycles of irrigation with a mixture of CBM water and low sodicity water (mixture: EC 3.1 mS cm^{-1} , SAR 13) followed by infiltration of rainfall-quality water (Bauder et al., 2008). The combination generated the high-SAR and low-EC conditions which can contribute substantially to swelling and dispersion of clay particles and result in loss of soil permeability (Bauder et al., 2008; Suarez et al., 2006).

Soil and water treatments for mitigating the soil effects caused by surface irrigation with CBM water have been tested. Gypsum ($\text{CaSO}_4 \cdot 2\text{H}_2\text{O}$) is a common soil amendment to ameliorate sodicity problems because it lowers SAR by providing Ca and raises EC through its high solubility (Gobran et al., 1982; Oster, 1982). Gypsum has been used with some success in the Powder River Basin (Brinck and Frost, 2009; Johnston et al., 2008). Better results have been obtained by altering the chemistry of CBM water by using sulfur burners and gypsum injection combined with application of gypsum and elemental sulfur to soil (Johnston et al., 2008). Despite additions of acidity and Ca, to irrigated fields, soluble salts periodically must be leached with excess irrigation water to remove Na accumulations in soils surface-irrigated with CBM water (Johnston et al., 2008). The amount of water provided by precipitation in the PRB may be insufficient for leaching of excess salt, as indicated by a study conducted two years after a single year of CBM surface water irrigation (31 cm CBM water; SAR = 24) (Johnston et al., 2011).

The deep SDI method described here is examined from the perspective of water balance and solute movement in the companion to this paper (Bern et al., 2012). The study of two sites found that the irrigation water is drawn upward into soil above the drip tubing, where evapotranspiration concentrates the associated solutes (Fig. 1). Excess water below the drip tubing keeps SDI solutes from concentrating there and leaches both SDI and native solutes toward the water table. Here we examine the geochemical patterns that six years of irrigation have imprinted upon an alfalfa field and a grass field at a single area by comparing them to non-irrigated soil from adjacent fields. Computer simulations were used to describe the geochemical interactions between irrigation water and soil. The goal is to show how conditions and processes are different in soil above and below the drip tubing, yet both develop relatively high

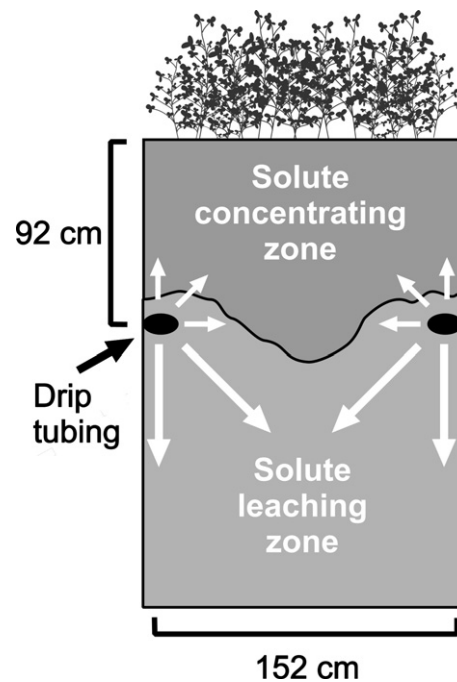


Fig. 1. Schematic depicting SDI system and generalized soil zones where different patterns of water and solute movement dominate. In the upper zone, solutes from the SDI system mix with dilute precipitation water but concentration by evapotranspiration dominates. In the lower zone, excess water maintains more dilute concentrations and leaches solutes downward. White arrows depict relative water movement from the drip tubing. The boundary between zones is depicted as a distinct black line, but is likely to be diffuse and difficult to identify in soil.

sodicity and low salinity. Previous studies have used coupled geochemical and unsaturated flow simulations to assess development of soil sodicity, but the calibration and assessment data typically come from column experiments (Jalali et al., 2008; Suarez et al., 2006). Here we use data from non-irrigated, control soils adjacent to SDI fields to simulate pre-irrigation soil conditions. The acidification of CBM water and its equilibration with soil is then simulated, along with evapotranspiration concentration of solutes and (below the drip tubing) transport of water and solutes downward with excess irrigation water. Results from the simulations are compared to geochemical properties of soil in the two fields irrigated for six years by the described SDI method. Understanding soil geochemical effects of this SDI method will improve the assessment of its impacts on soils of the Powder River Basin (Engle et al., 2011), and will also provide insight on the broader issue of using sodic waters for crop irrigation (Qadir and Oster, 2004).

2. Materials and methods

2.1. Site description and SDI operation

The Platmak SDI site is located ~14 km northeast of Sheridan, Wyoming at an elevation of ~1120 m. The regional climate is semi-arid with mean annual precipitation of ~370 mm and a mean annual temperature of ~7 °C (National Climatic Data Center). One of the SDI fields studied was planted with alfalfa (*Medicago sativa*) and the soil is mapped as a Zigweid–Kishona–Cambria complex (Soil Survey Staff). The other field is planted with grasses (*Dactylis glomerata* L., *Festuca arundinacea*, *Bromus biebersteinii*) and is mapped as Platmak loam, as are nearby non-irrigated, control soils (Soil Survey Staff). The alfalfa field studied is 2.9 ha in size and the grass field is 3.7 ha in size. The extent of SDI irrigation in the study area is 84 ha.

The site was not irrigated prior to installation of the SDI system. Daily irrigation via the SDI system began in January 2005 and had

been continuous through six growing seasons at the time of this study. CBM water is produced by gas wells year-round, and year-round irrigation is required to keep pace. The CBM water is delivered to a holding pond at the SDI site via pipeline. Degassing of CO₂ and other volatile compounds occurs at the pond. Subsequently, the water is acidified to approximately pH 6.0 by automated in-line addition of sulfuric acid. The target pH is 5.5, but there are technical challenges to in-line mixing of the viscous acid with water. Continuous acidification has been accomplished since about 2007. Disc filters removed particulate matter from the water, which was pumped to drip tubing beneath the fields. Depth and spacing of the drip tubing were selected by the operator on the basis of soil permeability, frost line, and crop characteristics (Zupancic et al., 2008). Polyethylene drip tubing is installed 92 cm below the surface and spaced 152 cm apart. Pressure-compensating emitters with a flow rate of 1 L min⁻¹ are spaced 92 cm apart along the tubing. A total of 8410 and 6600 mm of water were applied to the studied alfalfa and grass fields, respectively, between January 2005 and August 2010. Because of the limited life-span of both the produced water boom and the normal degradation of SDI infrastructure, the planned duration of irrigation for these fields is about a decade.

2.2. Sampling and analytical methods

2.2.1. Water sampling and analysis

Water samples were collected to determine the composition of CBM water supplied to the site, holding-pond water, and acidified irrigation water pumped to the fields. Quarterly sampling found little variation in the composition of CBM water over the course of six years of irrigation, a pattern that could be attributed to the water being a blend from nearly 1500 wells (BeneTerra LLC data). Water samples for this study were collected during each of four field visits in 2010. Temperature, specific conductance, and pH were measured in the field. Water samples for later analysis were collected in cleaned polyethylene bottles. Samples for chemical analysis were filtered to <0.2 μm, and aliquots for cation analysis were acidified with nitric acid. Samples for anion analysis were kept refrigerated and in the dark until analyzed. Unfiltered water samples were analyzed for alkalinity by titration using 1.6 N sulfuric acid (Hach Company, Loveland, CO, USA).

Cation and anion analyses were completed at the U.S. Geological Survey Laboratories in Denver, CO. Cation (Na, Ca, Mg, and K) concentrations were determined by inductively coupled plasma-mass spectrometry and SO₄²⁻, and Cl⁻ concentrations by ion chromatography (IC) at the U.S. Geological Survey in Denver. Standard reference samples (Woodworth and Connor, 2003) and standards prepared from laboratory reagents were analyzed alongside unknowns. Concentrations of reference samples and standards were within 10% of expected values. Charge-balance errors on all samples were <12%.

2.2.2. Soil sampling and mineralogical analysis

A land-surface-based electromagnetic geophysical survey of the Platmak grass and alfalfa fields and some adjacent non-irrigated land was completed in February 2010 (Burton et al., 2010). The resulting map of subsurface bulk soil electrical conductivity was used to select locations for soil sampling. Two groups of soil cores were collected, which were designated as “solitary” or “transect” cores. Three solitary soil cores were collected in the alfalfa field and three in the grass field. In both fields, solitary cores were collected at locations selected to represent high, low, and intermediate bulk soil electrical conductivity. The proximity of solitary cores to drip tubing was unknown. For the transect core sampling, a location of intermediate electrical conductivity was excavated in the alfalfa field to locate two adjacent lines of drip tubing. With those locations marked on the surface, three transect cores were collected

along a transect perpendicular to and at known distances from the drip tubing. Cores comprising the transect were collected with one essentially in line with the drip tubing, another halfway between the lines of drip tubing, and the last spaced evenly between those two cores. A second set of three transect cores was collected at approximately 7 m distance from the first transect along the same drip tubing. The process was repeated in the grass field. A total of 18 cores were collected from the grass and alfalfa fields (9 cores each). Five soil cores were collected at locations on non-irrigated land 40–150 m outside the SDI fields to serve as control sites.

Soil cores (45 mm in diameter) were collected in plastic liners from the alfalfa SDI, grass SDI, and non-irrigated control soils by using a hydraulic soil sampling, coring and drilling machine (Giddings Machine Company, Windsor, CO).¹ Cores were divided into 15-cm depth increments from 0 to 150 cm, and into 30 cm increments between 150 cm and bottom of the core, usually 450 cm. One set of alfalfa transect cores and two control cores were collected in February 2010. All other cores were collected in August 2010. Soil cores were split in the field and 469 samples were collected. Soil samples were air dried in the laboratory then disaggregated, sieved to <2 mm, and split by using a Jones splitter prior to analysis.

A subset of 76 soil samples from the February 2010 sampling was analyzed by quantitative X-ray diffraction (XRD) to determine mineral abundances. Samples were spiked with 20 wt.% corundum, micronized in isopropyl alcohol, sieved, and placed in side-packed powder mounts. Samples were scanned on either a PANalytical “X’Pert Pro-MPD X-ray Diffractometer or a Scintag X-1 Diffractometer”, and resulting spectra were processed by using the RockJock software, v. 11 (Eberl, 2003). The results of RockJock processing of XRD spectra were not normalized to 100%.

2.2.3. Soil chemical analysis

Chemical properties of 389 soil samples were analyzed by Servi-Tech Laboratories (Hastings, Nebraska). Soil carbonate content, reported as CaCO₃, was determined by measuring the pH of a mixture of acetic acid and soil (Loeppert et al., 1984). EC, pH and concentrations of Na, Ca, Mg, and K were determined for soil extracts at 1:1 water–soil weight ratio. The 1:1 water–soil ratio was selected for ease of comparison to computer simulations of soil extracts. To better assess total soil Na and gypsum content, water extractable Na and S were determined on samples extracted overnight at 20:1 water–soil ratios. Water extracts were separated from soil by using paper filters (Ahlstrom, #6420-0550) and elemental concentrations determined by inductively coupled plasma-atomic emission spectroscopy.

Concentrations of CO₂ in the subsurface air-filled pore space were measured in October 2010 at the eight coring locations in the alfalfa and grass SDI fields. Steel tubing 3.5 mm in diameter, with perforations on the sides near the tip, was pressed 75 cm deep into soil. The tubing was purged by drawing out two full volumes of gas and then a sample of soil gas was collected by using a 25 mL syringe. The concentration of CO₂ was measured in the field by injection of the sample into an EGM-1 infra-red gas analyzer (PP Systems, Amesbury, Massachusetts, USA).

2.3. Geochemical simulations

2.3.1. Simulation of irrigation water and pre-irrigation soil composition

Geochemical simulations were used to examine the interactions between irrigation water and soil. Four distinct scenarios of soil geochemistry (Tables 1 and 2) were simulated using the PHREEQC

¹ Any use of trade, firm, or product names is for descriptive purposes only and does not imply endorsement by the U.S. Government.

Table 1
Summary of pre-irrigation geochemical conditions in different simulated scenarios for SDI soil above and below the drip tubing.

Soil zone simulated	Scenario	Soil gypsum content	Water–soil ratio (g g ⁻¹)	EC (mS cm ⁻¹)	SAR	pH	ESP
Above drip tubing	1 – Gypsum absent	0%	0.12	0.9	1.8	7.1	3%
Above drip tubing	2 – Gypsum present	0.001–1.4%	0.12	2.9	0.8	6.8	1%
Below drip tubing	3 – Acidified irrigation water leaching	2.4%	0.14	5.1	10.6	7.0	14%
Below drip tubing	4 – Non-acidified irrigation water leaching	2.4%	0.14	5.1	10.6	7.0	14%

Table 2
Summary of parameters simulated in different scenarios for SDI soil above and below the drip tubing.

Soil zone simulated	Scenario	Advection/transport of SDI water?	Rain/snow infiltration?	SDI water acidified	SDI water evapotranspiration concentration factors
Above drip tubing	1 – Gypsum absent	No	Yes	Yes	1–15
Above drip tubing	2 – Gypsum present	No	No	Yes	1–7
Below drip tubing	3 – Acidified irrigation water leaching	Yes	No	Yes	1.0, 1.3, 1.65
Below drip tubing	4 – Non-acidified irrigation water leaching	Yes	No	No	1.0, 1.3, 1.65

software (version 2.18.3) with the Pitzer database (Parkhurst and Appelo, 1999).² Scenarios 1 and 2 refer to soil above the drip tubing, where evapotranspiration concentrates solutes to a greater degree. Scenarios 3 and 4 refer to soil below the drip tubing, where excess irrigation water transports solutes downward toward the water table (Fig. 1). All four models shared two common steps: simulation of the chemical composition of irrigation water, and simulation of the chemical composition of pre-irrigation soil water.

Water with the composition of mean CBM water delivered to the Platmak site (Table 3) was simulated to undergo degassing of CO₂, as it does in the holding pond. Then, acidification of the water to pH 6.0 by using sulfuric acid was simulated. Water temperature was assumed to change to a soil temperature of 10 °C upon application through the SDI system. Concentration of the solutes in irrigation water was then calculated to varying amounts of water loss by evapotranspiration. A selected range of solute concentration factors were used for each of the scenarios simulated.

Simulation of pre-irrigation soil water composition was based upon mean control soil composition between 30 and 90 cm deep for scenarios 1 and 2, and control soil between 90 and 450 cm deep for scenarios 3 and 4. Components included in the simulations were: soil mineral abundances, soil solution composition, cation exchange capacity, and composition of ions on exchange sites. Calcite, dolomite, and gypsum, were the phases considered to be reactive in the simulations. Calcite and dolomite concentrations were always sufficient to maintain saturation throughout all simulations. Calcite concentration was set to 3.6% and 1.8%, and dolomite set to 2.2% and 2.3%, above and below the drip tubing, respectively. Dolomite was considered only to dissolve, based upon unfavorable precipitation kinetics (Arvidson and Mackenzie, 1997). Gypsum presence and concentration varied across the four scenarios as described below.

Soil water composition in pre-irrigation soil was estimated by first entering into PHREEQC the mean composition of the 1:1 water–soil extracts from the control-site soil between 30 and 90 cm deep for scenarios 1 and 2, and between 90 and 450 cm deep for scenarios 3 and 4. Then removal of water relative to solutes was simulated to reduce the water–soil ratio from the 1:1 of the extract to represent the water content in control-site soil at the time of sampling. For scenarios 1 and 2, mean water content above 90 cm was used (0.12 g g⁻¹) (Bern et al., 2012). For scenarios 3 and 4

the mean water content between 90 and 450 cm deep was used (0.14 g g⁻¹). The resulting water composition was then equilibrated at 10 °C with the mean measured CO₂ concentration and soil minerals. Gypsum was omitted from this equilibration for scenario 1 (Table 1).

The relatively high abundance of 2:1 clay minerals found by the XRD analysis suggest that cation exchange capacity (CEC) will be high in soils at the study site. An average CEC per wt.% clay was calculated for the relevant soil series from the Soil Survey Geographic Database (Soil Survey Staff), and found to be 0.76 ± 0.17 cmol kg⁻¹ per wt.% clay (*n*=97). Soil above the drip tubing at the SDI site averages 36 wt.% clay and soil below the drip tubing averages 24%. Multiplying the two parameters yields an estimate of 27.0 cmol kg⁻¹ for the CEC of soil above the drip tubing (scenarios 1 and 2), and 18.2 cmol kg⁻¹ for the CEC of soil below the drip tubing (scenarios 3 and 4). For comparison, the average value measured on 36 sediment samples from another Powder River Basin site was 24.5 cmol kg⁻¹ (Healy et al., 2008). The abundance of Na⁺, K⁺, Ca²⁺ and Mg²⁺ ions on exchange sites was then determined by establishing exchange pool equilibrium with pre-irrigation soil water.

Simulation of ion equilibrium with cation exchange sites allows a calculation of the exchangeable sodium percentage (ESP). It should be noted that the water–soil ratio and other parameters will influence simulated ESP. Additionally, the affinities of the various cations for the types of exchange sites present on the suite of clay minerals and organic matter in Platmak site soils may be different than those used in the simulations. Therefore, ESP values from the simulations must be evaluated with caution.

2.3.2. Simulation of soil water above the drip tubing

Drier conditions are understood to draw irrigation water upward into soil above the drip tubing and evapotranspiration concentrates the solutes that accumulate there (Bern et al., 2012). Two scenarios were simulated for soil above the drip tubing. The scenarios differ in having gypsum be completely absent (scenario 1) versus having gypsum present in variable quantities (scenario 2) (Table 1). Gypsum concentrations ranging from 0.001% to 1.4% were used in scenario 2. Solute concentration factors, resulting from evapotranspiration, were varied within the scenarios. Factors ranging from 1 to 15 were used in scenario 1, and factors from 1 to 7 were used in scenario 2. The evaporatively concentrated, acidified irrigation water was added to soil at a ratio of 0.18 g g⁻¹, consistent with the average water content measured in SDI soil in August 2010. Compositions of water–soil extracts at 1:1 ratio were simulated for soils in scenarios 1 and 2 by computationally increasing

² PHREEQC input files for the specific geochemical simulations described are provided in an electronic supplement to this article.

Table 3
Average water chemistry for CBM water (n=4) and acidified CBM water (n=4) from Table 4 and water chemistry simulated by using PHREEQC as described in the text.

	EC ^a (mS cm ⁻¹)	pH	Alkalinity (mg L ⁻¹ as CaCO ₃)	Cl (mg L ⁻¹)	SO ₄ (mg L ⁻¹)	Ca (mg L ⁻¹)	K (mg L ⁻¹)	Mg (mg L ⁻¹)	Na (mg L ⁻¹)	SAR ^b
Averaged Platmak site waters										
CBM water	2.1	8.0	1204	8.5	<0.06	4.5	6.9	1.7	529	54
Acidified CBM water	2.6	5.9	223	9.1	972	5.1	7.4	1.7	568	57
Simulated waters										
CBM water	1.4	8.0	1204	8.5	0	4.5	6.9	1.7	529	54
Outgassed CBM water	1.4	9.3	1204	8.5	0	4.5	6.9	1.7	529	54
Acidified CBM water	1.6	6.0	327	8.5	841	4.5	6.9	1.7	528	54
Solute concentration factor 1.3	2.1	6.0	425	11.0	1093	5.8	9.0	2.2	687	61
Solute concentration factor 1.65	2.6	6.0	539	14.0	1388	7.4	11.4	2.8	872	69
Solute concentration factor 3	4.4	5.9	981	25	2522	13	21	5.1	1585	93
Solute concentration factor 7	9.4	5.9	2285	59	5878	31	48	12	3693	142
Solute concentration factor 15	17.7	5.8	4883	127	12,560	67	103	25	7892	208

^a Electrical conductivity.

^b Sodium adsorption ratio.

the water proportion in the soil solution, and adjusting temperature to 25 °C and setting CO₂ concentrations to 0.1%. Simulating 1:1 water extracts normalizes the results to a common soil water content and also allows direct comparison of simulation results to soil extract compositions measured in the laboratory.

An additional effect was tested for scenario 1. Ions present in soil solution were removed prior to simulation of the 1:1 water extract. Although solutes become concentrated during the growing season due to evapotranspiration, a portion of the same solutes are vulnerable to elution during deep soil wetting events that occur during the non-growing season. This simulation procedure generally duplicates the effect of dilute waters from rain or snowmelt infiltrating the soil and displacing or eluting soil water and the ions it contains. The solute concentrating step and solute eluting step have opposing effects on solute concentrations, but including both in the simulations is necessary because they are temporally distinct at the study site.

2.3.3. Simulation of soil water below the drip tubing

Scenarios 3 and 4 describe conditions in soil below the drip tubing where excess irrigation water is understood to result in leaching of soil (Bern et al., 2012). Scenarios 3 and 4 are identical, except that irrigation water is acidified in scenario 3, and left as unacidified CBM water in scenario 4. Comparison of the scenarios illustrates the effects of acidification.

Downward movement of water and solutes in scenarios 3 and 4 was simulated to occur by piston-flow and advection, the transport of solutes with the liquid water (Table 2). The column of soil through which this occurred in the simulation consisted of 30, 30-cm thick, 1-m² units of soil, representing the interval from about the depth of the drip tubing (90 cm) to an approximate water table depth of 960 cm. Irrigation water was added to the topmost soil unit (90 cm) at the mean water–soil ratio in SDI soil measured in August 2010 (0.27 g g⁻¹) and the solution associated with each unit was shifted downward to simulate downward movement by piston-flow. As solutions advanced they were equilibrated with the minerals and exchange pool in each successive unit.

Pore volumes of water passing through the top soil unit were calculated by converting estimates of excess irrigation water in the alfalfa field (1658 mm first year, 5048 mm six years) (Bern et al., 2012) to a kg m⁻² basis and dividing by the mass of water in a 30-cm thick, 1-m² unit of soil (116 kg). The simulations consider excess irrigation in the alfalfa SDI field, although excess in the grass SDI field is similar. Because of heavy irrigation rates at the start of the SDI operation, it is calculated that 14 pore volumes of irrigation water had passed through the top simulated soil unit in the first year. Therefore, 14 coupled transport/equilibration steps were simulated to describe the first year of leaching. Including the lower irrigation volumes in recent years, 44 transport/equilibration steps represented the six years of irrigation prior to soil sampling. To project future changes, 107 transport/equilibration steps were used to represent fifteen years of average excess water application.

An excess of irrigation water below the drip tubing suggests that irrigation water at those depths will be less concentrated by evapotranspiration, but the amount of concentration differs from two lines of analysis. Total water balance for the Platmak SDI site suggests that solutes should concentrate overall by a factor of 1.65 (Bern et al., 2012). In contrast, calculated aqueous Cl concentrations in SDI soil (8 ± 5 mg L⁻¹) beneath the drip tubing are quite similar to those in irrigation water, suggesting no solute concentration, or a factor of 1.0 (Bern et al., 2012). To accommodate both estimates simulations below the drip tubing were run using solute concentration factors of 1.0 and 1.65, as well as an intermediate factor of 1.3 (Table 2).

The simulation results and measured soil properties were compared by using the composition of 1:1 water–soil laboratory

extracts simulated from scenario 3 at two different transport/equilibrium steps. The water–soil ratio was adjusted to 1:1, temperature was set 25 °C, and CO₂ concentration was set to 0.1% to reflect laboratory conditions. Extracts were simulated for the topmost soil unit (90 cm depth) after the 14th (first year) and 44th (sixth year) transport/equilibration step. Extracts were simulated for the entire depth profile for the sixth year to coincide with sample collection at the Platmak site.

3. Results

3.1. Analytical results

3.1.1. Water chemistry

CBM water pumped to the Platmak site was Na-HCO₃ type and had EC ranging from 2.0 to 2.2 mS cm⁻¹ (Table 4). The CBM water at the Platmak site contains slightly higher concentrations of Na and lower concentrations of Ca and Mg than average CBM water found in the Powder River Basin (Rice et al., 2002). As a result, the SAR values (48–59) are at the high end of the expected range. The combination of EC and SAR place the water slightly beyond the severe restriction category and therefore this water poses a significant risk of soil degradation even with specially designed cropping management (Ayers and Westcot, 1985). Concentrations of SO₄²⁻ are <0.06 mg L⁻¹ and Cl is present in concentrations between 7 and 10 mg L⁻¹.

Water in the storage pond has higher pH than the supplied CBM water due to CO₂ outgassing (Table 4). Higher SO₄²⁻ concentrations in the pond are attributed to return of acidified water from flushing of the SDI filtration system. The water delivered to the fields reflects in-line acidification by H₂SO₄. The target pH is 5.5, but values can range from 5.5 to 6.1 (Table 4). After acidification, irrigation water is altered to be a Na-SO₄ type; the SAR is unchanged.

3.1.2. Mineral abundances

Notable differences in the mineral composition of SDI and control soils were not apparent in the XRD results. The sum of crystalline materials identified in samples averaged a total of 91 ± 2 wt.%. One contributing factor to low totals is the presence of X-ray amorphous material, including organic carbon in general and visible quantities of lignite in particular. Major silicate minerals showed little systematic variation with depth, and averaged abundances are presented. Quartz is the most abundant (41 ± 5 wt.%) mineral, and a suite of clay minerals account for 34 ± 6 wt.% of the soil. Among these clay minerals, illite/muscovite phases dominate (18 ± 3 wt.%), followed by smectite (7 ± 2 wt.%), kaolinite (6 ± 1 wt.%), and chlorite (4 ± 1 wt.%) (Table 5). Feldspar content averages 8 ± 1 wt.% and includes potassium feldspar and plagioclase.

In contrast to the silicate minerals, abundances of calcite and dolomite (CaMg(CO₃)₂) varied systematically with depth (Fig. 2). Calcite and dolomite generally are not detected in soil 0–15-cm deep, and at some sites are also absent from soil 15- to 30-cm deep. Many of the highest calcite concentrations, up to 7.8%, were found between the 30- and 60-cm depth, which are interpreted to be pedogenic calcite accumulation or redistribution (Fig. 2a and c). Below the 60-cm depth, calcite concentrations vary widely (0.3–9.1%). In contrast, most dolomite concentrations below the 60-cm depth are between 2 and 3% (Fig. 2b and d).

Total carbonate concentration measured by the acetic acid method correlated well with the sum of calcite and dolomite concentrations measured by XRD ($R^2 = 0.92$, $p < 0.01$). The acetic-acid method always estimated carbonate mineral content in excess of calcite as determined by XRD, but less than combined calcite and dolomite. The discrepancy is likely due to incomplete dolomite

Table 4
Measured properties of waters at the Platmak SDI site.

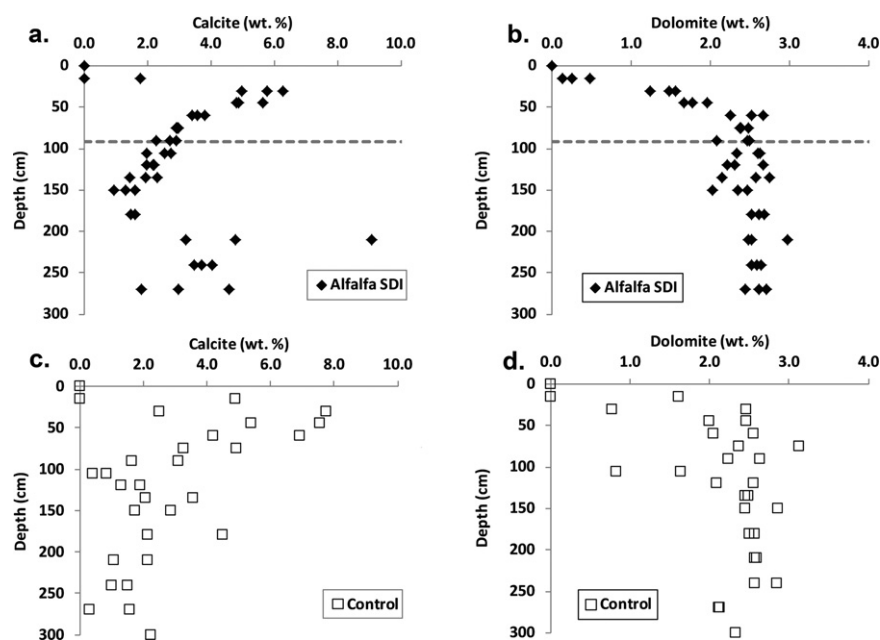
Sample type	Collected	Temperature (°C)	Conductivity (mS cm ⁻¹)	pH	Alkalinity (mg L ⁻¹ as CaCO ₃)	Cl (mg L ⁻¹)	SO ₄ (mg L ⁻¹)	Ca (mg L ⁻¹)	K (mg L ⁻¹)	Mg (mg L ⁻¹)	Na (mg L ⁻¹)	SAR ^a
CBM water	17-Feb-2010	11.2	2.2	8.0	1272	8.0	<0.06	3.2	4.4	1.7	558	59
CBM water	27-May-2010	18.4	2.2	8.0	1228	10	<0.06	4.8	6.4	2.0	585	57
CBM water	10-Aug-2010	23.3	2.0	7.9	1117	8.6	<0.06	5.7	1.1	1.5	517	50
CBM water	14-Oct-2010	20.3	2.1	8.0	1198	7.1	<0.06	4.3	5.8	1.5	454	48
Holding pond	17-Feb-2010	6.3	2.3	8.1	1171	9.1	91	3.2	4.5	1.8	538	59
Holding pond	27-May-2010	23.0	2.2	8.6	1127	9.4	71	4.7	6.6	2.1	571	55
Holding pond	10-Aug-2010	27.3	2.2	8.4	1046	9.2	82	4.4	1.1	1.5	527	55
Holding pond	14-Oct-2010	17.0	2.2	8.1	1137	8.1	91	4.8	3.3	1.5	564	57
Acidified water	17-Feb-2010	7.6	2.6	6.1	281	10	944	5.2	5.7	1.8	510	49
Acidified water	27-May-2010	18.5	2.5	6.0	217	9.2	904	4.8	5.9	2.0	636	68
Acidified water	10-Aug-2010	25.4	2.5	5.5	106	8.9	1090	5.8	14	1.7	549	52
Acidified water	14-Oct-2010	15.5	2.5	6.1	288	8.0	950	4.7	3.6	1.5	576	59

^a Sodium adsorption ratio.

Table 5

Clay mineral abundances as determined by quantitative X-ray diffraction on select samples of control and alfalfa SDI soil from the February 2010 sampling.

	Illite/muscovite (%)	Smectite (%)	Kaolinite (%)	Chlorite (%)	Total clay minerals identified by XRD (%)
Mean and standard deviation	18.0 ± 3.0	7.1 ± 2.4	5.8 ± 1.3	3.6 ± 0.8	34.5 ± 6.1
Range	11.7–27.2	2.9–14.0	3.2–9.6	2.2–5.7	22.4–51.6

**Fig. 2.** Soil mineral content as determined by quantitative X-ray diffraction on select samples from the February 2010 sampling: (a) calcite in alfalfa SDI soil; (b) dolomite in alfalfa SDI soil; (c) calcite in control soil; (d) dolomite in control soil. Horizontal dashed lines show the 92-cm-depth of drip tubing in SDI fields.

dissolution by the acetic-acid method. Measurements of total carbonate between 30 cm and 450 cm deep by the acetic acid method ranged from 1.7 to 15.5 wt.% CaCO_3 . Based on the XRD and acetic acid results, calcite and dolomite are consistent constituents of the soil below the 30-cm depth.

Gypsum abundance also varies with depth. Gypsum measured by XRD ranged from not detected to 6.6 wt.%. The accuracy of the technique is questionable at low gypsum concentrations (<1 wt.%). To estimate the abundance of gypsum in samples with low concentrations, XRD results were examined by comparing the gypsum content to that estimated by 20:1 water–soil extractions. Regression of concentration estimates from the two techniques found good correlations for both SDI-irrigated ($R^2 = 0.99$, $p < 0.01$, slope = 0.95) and control soils ($R^2 = 0.98$, $p < 0.01$, slope = 0.84). Based upon the consistency of the two methods for most samples, the 20:1 water extractable sulfur data is used to estimate soil gypsum content. Soil less than 90-cm-deep generally contains little gypsum, while deeper soil has widely variable, but greater concentrations (Fig. 3). Based upon water-extractable sulfur, soil gypsum concentrations deeper than 90-cm ranged from 0.1 to 12 wt.%, and averaged 2.1 ± 1.8 wt.% for SDI soil and 2.4 ± 1.7 wt.% for control site soil (Fig. 3). Stringers and nodules of gypsum were visible in samples with greater gypsum concentrations. In contrast, gypsum concentrations in soil less than 90 cm deep ranged from 0.02 to 8.6 wt.% and averaged 0.2 ± 0.4 wt.% for SDI soil and 0.5 ± 1.9 wt.% for control site soil.

3.1.3. Composition of soil extract solutions³

The EC of 1:1 water soil extracts show common patterns in control and SDI soils. Above about the 90-cm depth, EC of control soil extraction solution is rarely greater than 0.5 mS cm^{-1} and alfalfa SDI soil is rarely greater than 1.2 mS cm^{-1} (Fig. 4). Grass SDI soil has more variability, with a few samples $>2 \text{ mS cm}^{-1}$ but the majority are below that value (Fig. 4). In contrast, control soil samples below the 90-cm depth have 1:1 solution EC mostly $>2 \text{ mS cm}^{-1}$ and range up to 6 mS cm^{-1} . Alfalfa and grass SDI soils also have values $>2 \text{ mS cm}^{-1}$ for the majority of samples below the 90-cm depth, and range up to 4.9 mS cm^{-1} . The EC of the 1:1 water–soil extracts were correlated with concentrations of sulfur extracted at 20:1 water–soil ratio from all soil types ($R^2 = 0.60$, $p < 0.01$). The correlation between EC and extractable sulfur might be higher except for the suggestion of gypsum saturation in some 1:1 extracts. Correlation of EC with extractable sulfur, and extractable sulfur with gypsum, indicates that gypsum presence is a major control on EC.

The pH values of 1:1 water–soil extracts in control soils fall generally in the range of 7.3–8.4, with a few lower values in near-surface soil, and a few higher values near the 45-cm depth (Fig. 4). By comparison, SDI soils have higher pH values, ranging generally from 7.4 up to 9.1, and again the lowest values were measured on soils from near the ground surface.

SAR values of 1:1 water–soil extracts from SDI soils clearly show the effects of irrigation with high-SAR water when compared to SAR values of non-irrigated control soils (Fig. 5). Control soil 0–30 cm deep had SAR values of 0.1–0.5. SAR values are only slightly higher in alfalfa and grass SDI-irrigated soils between 0- and 30-cm depth, ranging from 0.5 to 0.7 and 0.3 to 1.2, respectively. Below that depth, SAR values of alfalfa and grass SDI soils rise abruptly, while control soils change little. In alfalfa SDI soil, SAR values range up to 13, with higher values common in the 45–135-cm depth interval.

³ Soil chemistry data are provided in an [electronic supplement](#) to this article.

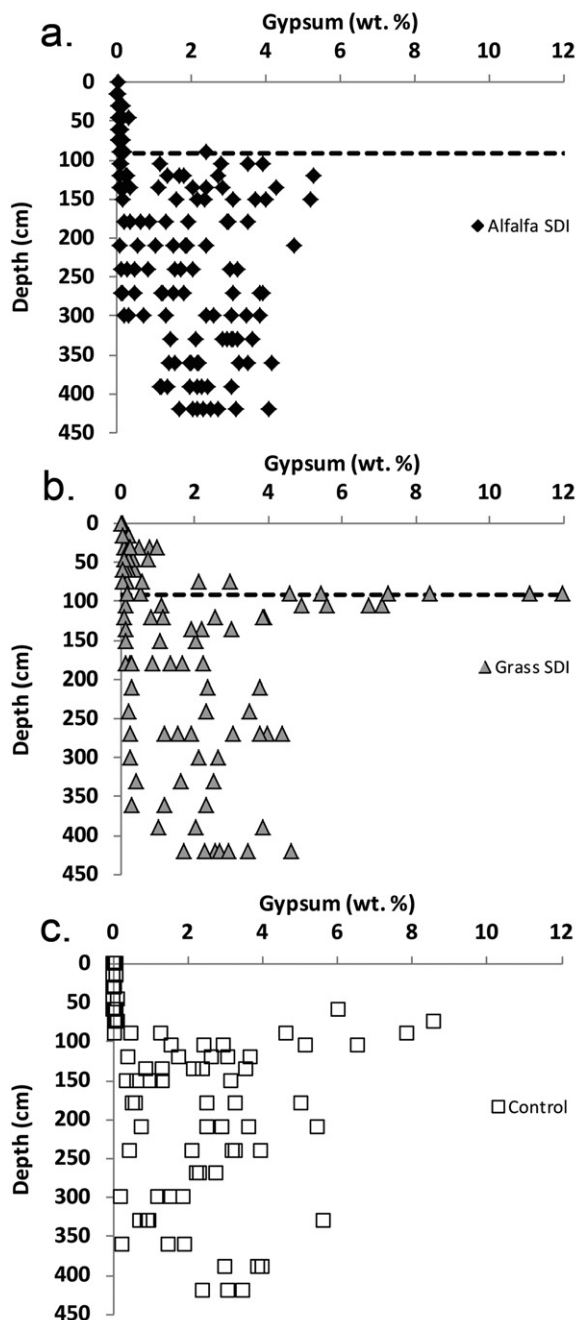


Fig. 3. Estimated weight percent gypsum concentrations, calculated from water-extractable sulfur as described in the text: (a) alfalfa SDI soil; (b) grass SDI soil; (c) non-irrigated control soils. Horizontal dashed lines show the 92-cm-depth of drip tubing in SDI fields.

In grass SDI soil, SAR values range up to 12.8, and the highest values are most common in the 30–105-cm depth interval. A marked decline in SAR to values between 2 and 4 in the deeper portions of the SDI soil profiles is associated with the increases in EC and extractable sulfur and is attributable to gypsum dissolution.

Na extracted at 20:1 water–soil ratio may be an incomplete measure of water-soluble Na in soil because some Na would be retained on cation exchange sites. However, dissolution of gypsum and calcite in the samples provides additional Ca^{2+} ions to exchange for Na^+ , making the Na^+ extraction more complete. Therefore, Na extracted at 20:1 water–soil ratio seems a reasonable estimate of total water soluble Na. Control soils contained 20–49 mg kg^{-1} Na in

the top 45 cm (Fig. 5). Sodium concentrations are larger at greater depths, ranging up to 395 mg kg^{-1} Na. By comparison, SDI soils contained slightly more Na in the 0–30 cm-depths, ranging from 54 to 87 mg kg^{-1} Na for alfalfa SDI soil and 34–168 mg kg^{-1} Na for grass SDI soil. Substantially greater Na concentrations in SDI soil compared to control soil are more apparent below 30 cm depth grass SDI soil and at 45 cm depth in alfalfa SDI soil (Fig. 5). Maximum Na concentrations in the alfalfa SDI soil occur at and below the drip tubing and range up to 747 mg kg^{-1} . In grass field samples maximum Na concentrations are found above the drip tubing where they range up to 834 mg kg^{-1} .

Using bulk density data from Bern et al. (2012), Na extracted at 20:1 water–soil ratio totals 3.0 ± 0.2 and $2.8 \pm 0.1 \text{ kg m}^{-2}$ for the 0–450-cm depth interval in the alfalfa and grass SDI fields, respectively. Control soil contained $1.1 \pm 0.4 \text{ kg m}^{-2}$ of Na in the same interval. Above the drip tubing, Na extracted at 20:1 water–soil ratio totals 0.50 ± 0.07 and $0.68 \pm 0.11 \text{ kg m}^{-2}$ for the alfalfa and grass SDI fields, respectively. Control soil contained $0.13 \pm 0.07 \text{ kg m}^{-2}$ of Na in that same interval. For comparison, the irrigation water has added 4.6 and 3.6 kg m^{-2} of Na to the alfalfa and grass fields, respectively (Bern et al., 2012).

Irrigation water has the potential to add SO_4 to SDI soil, due to acidification with sulfuric acid, but also can potentially leach SO_4 from the starting soil composition as a result of gypsum dissolution. If acidification had been consistent over the operation of the SDI system, approximately 8.2 and 6.4 kg m^{-2} of SO_4 would have been added to the alfalfa and grass fields, respectively. Assuming all 20:1 water extractable sulfur was present as SO_4 , control soil contained $74 \pm 13 \text{ kg m}^{-2}$ of water extractable SO_4 in the 0–450 cm interval. By comparison, total water extractable SO_4 was lower in the alfalfa ($57 \pm 14 \text{ kg m}^{-2}$) and grass ($69 \pm 22 \text{ kg m}^{-2}$) SDI fields.

The concentration of CO_2 in soil gas at the 75-cm depth in October 2010 averaged $3.9 \pm 1.1 \text{ vol.}\%$ (1 S.D.) without significant differences between the grass and alfalfa fields ($p=0.74$, two-sample Kolmogorov–Smirnov test).

3.2. Simulation results

3.2.1. Simulated irrigation water and pre-irrigation soil composition

The concentration of solutes in water is a major influence on the simulated interactions between water and soil. Both EC and SAR increase with water removal by evapotranspiration (Table 3). Acidification of the CBM water slightly increases its EC, but has little effect on SAR (Table 3). No effects from plant uptake or release of ions are included in the simulation of evapotranspiration.

Table 1 presents geochemical attributes of soil water in pre-irrigation soil for the four simulated scenarios. Compared to concentrations measured in 1:1 water–soil extracts from control soil, EC and SAR are higher in the simulated pre-irrigation soil water. The differences are attributed to higher concentrations of ions in control soil water, reflecting the low water–soil ratios. Lower pH reflects the higher CO_2 concentrations measured in SDI fields ($3.9 \pm 1.1\%$) compared to conditions for laboratory extracts.

3.2.2. Simulated soil water above the drip tubing

Two major patterns emerge from the simulations of soil water above the drip tubing. First, scenario 1 (gypsum-absent) and scenario 2 (gypsum-present) evolve to have distinctly different compositions. This is evident in the lack of overlap in plots of EC versus SAR, and EC versus pH for the 1:1 water–soil extracts for the two scenarios (Fig. 6a and b). Greater EC in scenario 2 is attributed to gypsum dissolution. The Ca^{2+} released from gypsum directly decreases SAR but also decreases pH by suppressing dissolution of calcite and dolomite. Second, increases in the solute concentration factor, resulting from evapotranspiration, consistently increases

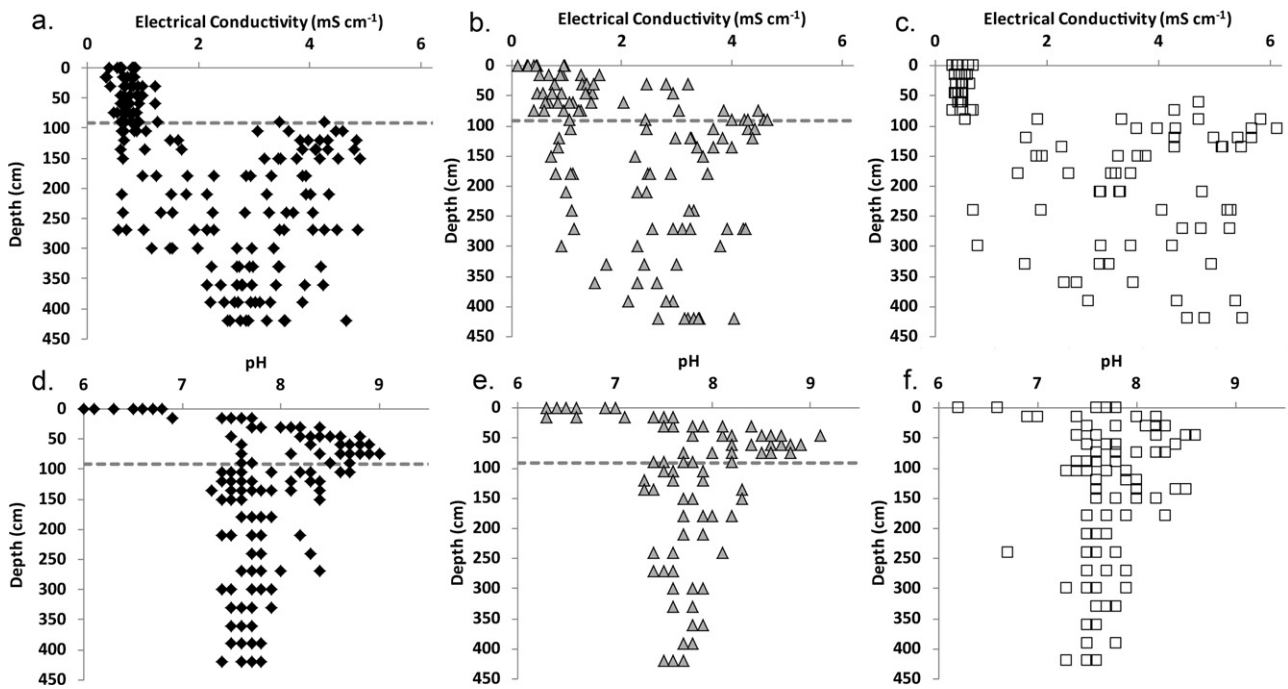


Fig. 4. Chemistry of 1:1 water–soil extracts from the Platmak SDI site plotted by depth: (a–c) electrical conductivity for alfalfa SDI, grass SDI and control soils, respectively; (d–f) pH for alfalfa SDI, grass SDI and control soils, respectively. Horizontal dashed line in plots for alfalfa and grass SDI soils represent the depth of the drip tubing.

SAR for soil (Fig. 6a). Nonetheless, soil SAR is dramatically lower compared to that predicted by direct evaporation of irrigation water prior to interaction with soil. SAR values for simulated irrigation waters with solute concentration factors of 1, 7, and 15 are 54, 142, and 208, respectively (Table 3), while no simulated 1:1 water–soil extract SAR values exceed 14. The lower SAR arises from adsorption of some Na^+ on exchange sites and release of Ca^{2+} and Mg^{2+} from soil minerals.

The effect of soil water flushing by infiltration of rain and snowmelt is apparent in scenario 1. Flushing displaces the soil water, which was derived from evapotranspiration-concentrated irrigation water. EC decreases in that portion of the soil because the concentrated ions contained in the soil water are transported in the eluting water. In contrast, the SAR changes little, because Na^+ is on exchange sites is released as new water releases Ca and Mg from carbonate mineral dissolution.

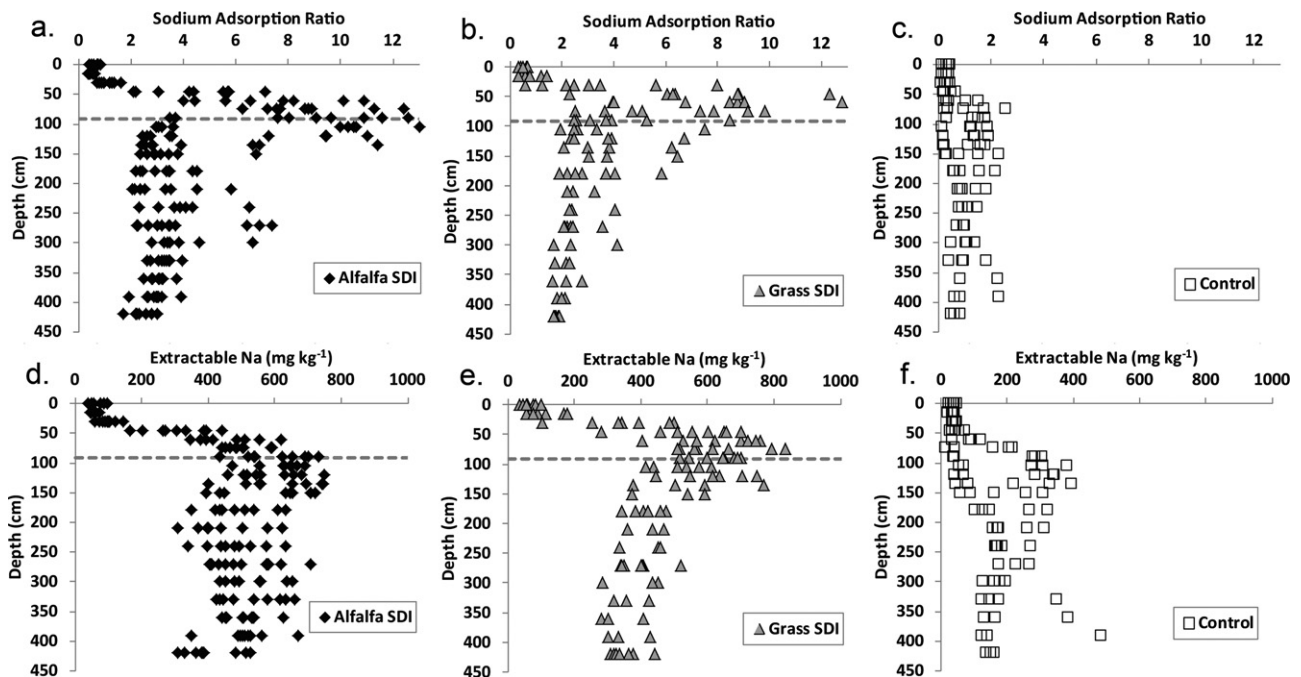


Fig. 5. Measures of Na abundance at the Platmak SDI site plotted by depth: (a–c) sodium adsorption ratios for 1:1 water–soil extracts alfalfa SDI, grass SDI and control soils, respectively; (d–f) Na extracted by 20:1 water–soil extracts and expressed on a dry mass basis for alfalfa SDI, grass SDI and control soils, respectively. Horizontal dashed line in plots for alfalfa and grass SDI soils represent the depth of the drip tubing.

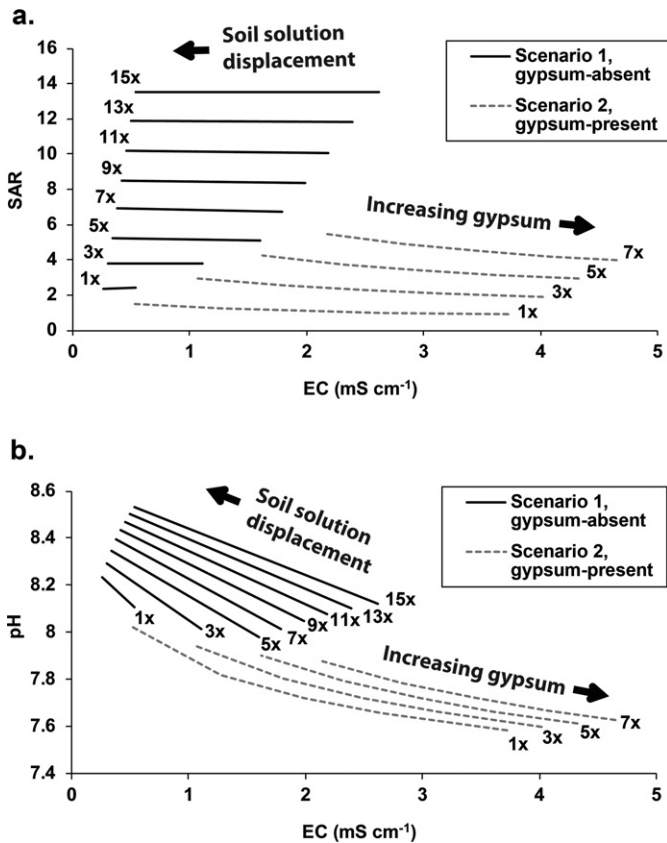


Fig. 6. Comparisons of output values for simulations of SDI soil above the drip tubing in scenarios 1 and 2: (a) EC and SAR in simulated 1:1 extracts; (b) EC and pH in simulated 1:1 extracts. Scenario 1 (gypsum-absent) varied the displacement of ions in soil solution, simulating flushing by infiltrating rain or snowmelt. Scenario 2 (gypsum-present) varied the amount of gypsum present in soil. Both scenarios varied the factor by which evapotranspiration concentrated the acidified CBM water and those factors are indicated next to lines marking their chemical trends.

Scenario 2 varies the amount of gypsum present from trace amounts (0.001%) up to that sufficient to achieve gypsum saturation in a 1:1 water–soil extract (1.4%). Varying gypsum concentration has relatively little influence on SAR, but substantially affects the EC. Further, SAR values for a given evapotranspiration factor are lower in scenario 2 by only about 1–2, compared to the scenario 1. The minimal effects of gypsum on SAR can be attributed to the precipitation of calcite resulting from reaction of Ca²⁺ supplied by gypsum dissolution and available carbonate species. Calcite is predicted to form as gypsum dissolves, resulting in decreasing pH and alkalinity with increasing gypsum. All solutions simulated for scenarios 1 and 2 are slightly to moderately oversaturated relative to dolomite, with saturation indices ranging up to 0.5. Inhibiting dolomite precipitation in the simulations results in retention of Mg in solution, and consequently lower SAR values.

Simulation results for soil above the drip tubing compare favorably to measured EC and SAR values in 1:1 water–soil extracts (Fig. 7). Samples of irrigated soil between 30 and 120 cm deep have combinations of EC and SAR values that fall almost entirely within the domains described by scenarios 1 and 2. Soil down to the 120-cm depth is included in the assessment because the transition between soil zones is not expected to be abrupt (Fig. 1). Most measured values fall in the gypsum-absent (scenario 1) domain, as would be expected based upon the lack of gypsum in this zone in both SDI and control soil (Fig. 3). Most samples from alfalfa SDI soil have low EC values that indicate displacement of soil solution ions, indicating that periodic flushing by rain and snowmelt is an important process in those soils. Grass SDI soil has more scatter within the

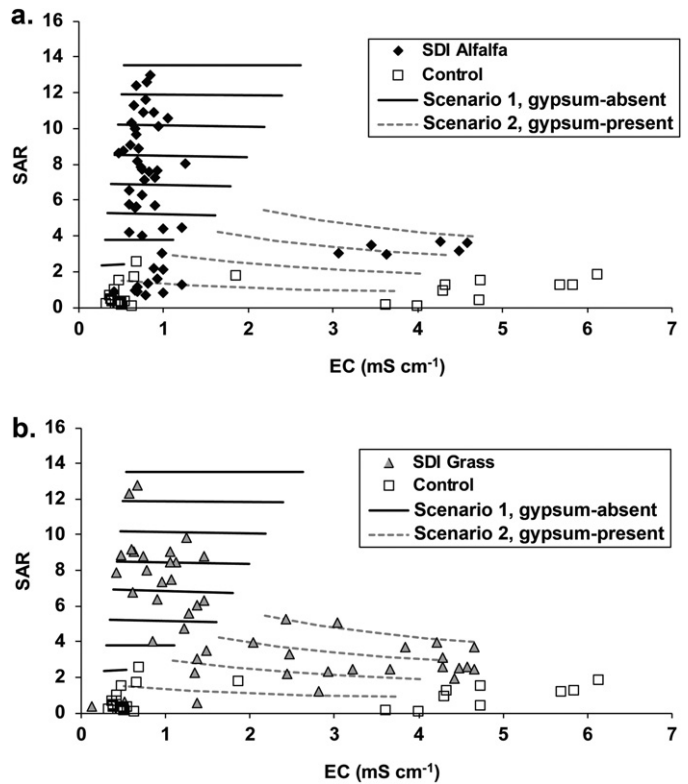


Fig. 7. Plots of EC and SAR of 1:1 water–soil extracts for samples from between 30 and 120 cm deep: (a) alfalfa SDI soil; (b) grass SDI soil. Control soil values for the same span of depths are shown for comparison. The EC and SAR results from geochemical simulation scenarios 1 and 2 of soil above the drip tubing depicted in Fig. 6a are shown for comparison.

gypsum-absent domain, possibly indicating less flushing. The highest SAR values measured in soil samples fall within the scenario 1 domain and range up to >13, compared to measured SAR values ranging up to ~7 in the scenario 2 domain (Fig. 7). The correspondence of low solute concentration factors and gypsum presence is consistent with the greatest abundance of gypsum occurring below the 90-cm depth (Fig. 3) where less evaporative concentration of SDI solutes would be predicted. Both alfalfa and grass SDI soils are predicted to have SAR values >12 in the scenario 1 domain, for which the simulations indicate a solute concentration factor of >13. The ESP indicated for those samples by the simulations is >15%.

A plot of EC and pH measured values on 1:1 water–soil extracts shows that they do not fall perfectly within the domain of simulated values (Fig. 8). However, where differences exist, they are generally less than 0.4 pH units. Irrigation with unacidified water would generate pH values greater than those seen with acidified water in scenarios 1 and 2. High pH values measured in 1:1 extracts may therefore be detecting lapses in acidification that have been noted by the operator and were more common in early years of operation.

3.2.3. Simulated soil water below the drip tubing

Geochemical simulations of soil-water composition below the drip tubing in scenarios 3 and 4 include downward movement of excess irrigation water which results in solute leaching. To simulate the transport of solutes temporal and spatial components were included in the modeling. Scenarios 3 and 4 also assume a constant and relatively high ratio of irrigation water to soil. For that reason we initially examine changes in soil water composition, rather than extracts, through the simulations. Results from the simulations using a solute concentration factor of 1.3 are described; other factors (1.0 and 1.65) were considered in the calculations to

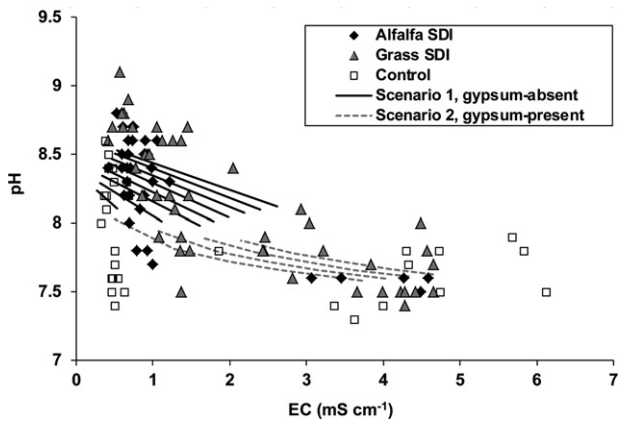


Fig. 8. Plot of EC and pH for 1:1 water–soil extracts for samples from between 30 and 120 cm deep from alfalfa SDI, grass SDI, and control soils. The EC and pH results from geochemical simulation scenarios 1 and 2 of soil above the drip tubing depicted in Fig. 6b are shown for comparison.

provide a measure of the evapotranspiration concentration factor's influence.

Scenario 3 simulates irrigation water acidified to pH 6.0. The uppermost soil unit in the simulation is positioned at the drip tubing and the chemical changes there are similar to changes that happen in deeper units. Simulated pre-irrigation soil water in the uppermost unit has a SAR of 10.6 and EC of 5.1 mS cm^{-1} . Concentration of solutes in the irrigation water by a factor of 1.3 produced a SAR of 61 and an EC of 2.1 mS cm^{-1} (Table 3). Equilibration of this solution with soil during early steps of the simulation, yields a SAR of 7 and EC of $\sim 4.1 \text{ mS cm}^{-1}$ in the new soil water (Fig. 9). The change in composition as irrigation water becomes soil water is largely driven by gypsum dissolution. However, unlike the simulations of soil above the drip tubing, dolomite dissolution plays a more significant role. While gypsum and dolomite dissolve, calcite precipitates from Ca^{2+} released by gypsum and dolomite. A lower SAR in soil water derived from high-SAR irrigation water, compared to native soil water, is attributed to lower dissolved Na concentrations in the irrigation water, as both waters equilibrate with the same soil minerals.

Downward transport of solutes by excess irrigation water eventually results in depletion of gypsum in the uppermost simulated soil unit. Modeling predicts the depletion is complete before the end of the second year of simulated irrigation, and the effects on pH, EC and SAR are pronounced by the sixth year (Fig. 9). Without gypsum, soil-water EC declines abruptly to around 2.4 mS cm^{-1} and SAR values rise. The rise in SAR is tempered initially by exchange of Na^+ for Ca^{2+} and Mg^{2+} on cation exchange sites. Eventually, exchangeable Ca^{2+} and Mg^{2+} are depleted by continued downward flow of excess irrigation water and SAR rises to >14 (Fig. 9). Following gypsum depletion, calcite continues to form from Ca^{2+} supplied from exchange sites, but at a decreasing rate for several more transport/equilibrium steps. With depletion of exchangeable Ca^{2+} , calcite begins to dissolve. The decline in calcite precipitation and subsequent dissolution both cause the pH of soil water to increase (Fig. 9) and dissolution of dolomite to decrease. Under these conditions, the limited calcite and dolomite dissolution are the only processes acting to lower the SAR of irrigation water. Only after gypsum is depleted in the overlying soil unit above does substantial gypsum dissolution begin in the unit below. This predicts that the effects of gypsum depletion will proceed sequentially down the simulated soil column.

Model results generated by using the 1.65 and 1.0 solute concentration factors bracket those obtained from the 1.3 factor. The higher concentration factor of 1.65 generates higher EC, SAR,

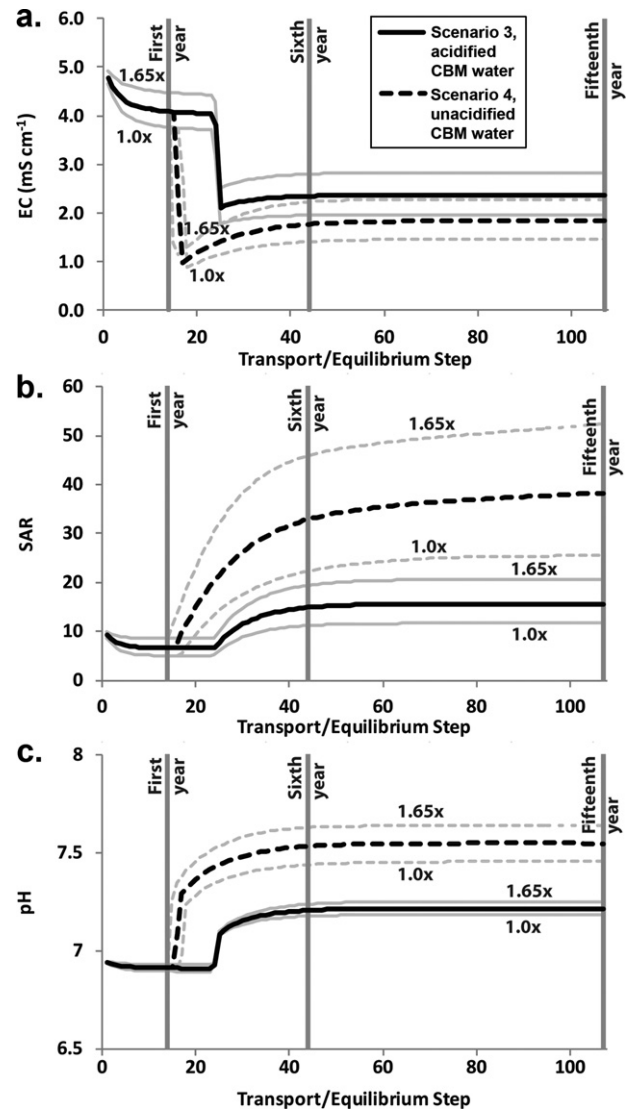


Fig. 9. Changes in the soil water composition of the uppermost soil unit (90–120 cm depth) for geochemical simulations of soil below the drip tubing, scenarios 3 and 4: (a) EC and transport/equilibrium step; (b) SAR and transport/equilibrium step; (c) pH and transport/equilibrium step. Scenario 3 (CBM water acidified to pH 6.0 with sulfuric acid) and scenario 4 (unacidified CBM water) are distinguished in the legend. Simulations using a solute concentration factor of 1.3 for irrigation water are plotted as black lines, while simulations using factors of 1.0 and 1.65 are shown as gray lines and labeled in the figure. Steps corresponding to the simulated first, sixth, and fifteenth year of irrigation at the SDI site are labeled. Abrupt breaks in the trends mark the step where gypsum is fully depleted from the model unit.

and pH values, and the 1.0 factor predicts lower values for these parameters (Fig. 9). For simulations of acidified irrigation water, the effect of solute concentration is particularly noticeable for SAR after gypsum depletion. In that situation, SAR rises to 21 when using the 1.65 factor, but only 12 using the 1.0 factor. Although the simulated ESP values must be evaluated with caution, they provide a broad indication of the changes caused by the sodic water. ESP is 7, 9, 12% for the concentration factors 1.0, 1.3 and 1.65, respectively, in simulated soil while gypsum is present. After gypsum depletion the ESP values are predicted to increase to 15, 20 and 25%, respectively.

Simulation of irrigation with unacidified CBM water in scenario 4 generally yields lower values of soil-water EC and higher values of pH and SAR (Fig. 9). In this scenario, abundant bicarbonate in unacidified water combines with Ca^{2+} ions released as gypsum dissolves to precipitate calcite. Greater calcite precipitation increases gypsum dissolution and gypsum is depleted more quickly. As a

result, changes in soil water composition associated with gypsum depletion are predicted for the uppermost soil unit early in the second year of irrigation, rather than late in the second year (Fig. 9). After 15 years of simulated irrigation with unacidified water and a concentration factor of 1.3, a 180-cm-thick section (6 modeled soil units) is depleted of gypsum compared to a 120-cm-thick section (4 modeled soil units) with acidified water. In the gypsum-depleted units, leached by unacidified irrigation water, soil-water EC is 1.8 mS cm^{-1} and SAR is 33 after six years of irrigation (Fig. 9) while ESP is 55%. Such values would be expected to cause notable reductions in soil hydraulic conductivity (McNeal and Coleman, 1966). With continuing irrigation, SAR and ESP continue to increase, ultimately reaching 38 and 60%, respectively. Using the 1.0 and 1.65 concentration factors will yield a range of SAR values from 22 to 46 and EC from 1.4 to 2.2 mS cm^{-1} after six years of irrigation. The higher-SAR lower-EC conditions in these scenarios are driven largely by the higher pH and alkalinity of unacidified water, which suppress carbonate mineral dissolution after gypsum depletion.

Returning to scenario 3, simulations of 1:1 extract solution EC, pH, SAR and extractable Na at the sixth-year time step are plotted in Fig. 10. Measured values from samples of control and alfalfa SDI soil below 90-cm depth are plotted for comparison. The variability in measured values contrasts with the simple patterns generated by the simulations. This is to be expected as patterns of unsaturated flow through the heterogeneous soil are likely to be temporally and spatially complex. The simulations, by comparison, consist of uniform and unidirectional flow along with a requirement to achieve chemical equilibrium prior to transport. Additionally, gypsum content in the studied soils is quite variable (Fig. 3), and the same is likely true for CEC, whereas uniform values were used for all soil units at the start of the simulations. Nonetheless, measured EC tends to be lowest and pH and SAR generally have their highest values in the 100–150-cm zone immediately below the drip tubing, as predicted by in the simulations. Measured 1:1 water–soil extractable Na concentrations throughout the lower profile are generally bracketed by the simulations using different solute concentration factors. Overall, the modeled values compare favorably with measured values and the model explains basic spatial patterns observed in soil composition.

In addition to sodicity, root zone salinity is a concern for long-term sustainability of the irrigation method described here. Application of water in excess of crop demand keeps salinity lower near the application point, but computer simulations suggest that solutes will accumulate above the drip tubing over time (Bern et al., 2012). Alfalfa yields can decline when soil salinity exceeds 2.0 mS cm^{-1} , as assessed by soil saturated pastes (Maas and Grattan, 1999), some bromes and fescues are moderately tolerant of salinity, but *Dactylis glomerata* yields can decline when soil salinity exceeds 1.5 mS cm^{-1} (Maas and Grattan, 1999). Considering the EC measured above the drip tubing in 1:1 water–soil extracts (Fig. 4), salinity in the rooting zone should be monitored relative to these thresholds. The issue could become more acute when the SDI system is shut down; in the absence of irrigation water, natural precipitation rates may be too low to flush accumulated solutes from the soil zone. As a result, salinity of soil water may increase.

4. Discussion

Addition of Na to the SDI soils via irrigation water from the drip tubing buried 92 cm deep has not resulted in large Na enrichments in the shallowest portions of the Platmak alfalfa or grass SDI fields. This is evident in both the SAR values and total water extractable Na measured in SDI soil 0–30 cm deep (Fig. 5). This is in sharp contrast to sites using CBM waters for surface irrigation

elsewhere in the Powder River Basin, where the highest SAR values are found at and near the soil surface (Ganjegunte et al., 2005, 2008). High sodicity and low salinity at the soil surface can cause clay swelling and dispersion and thereby reduce infiltration rates as well as cause problems with crusting, aeration, and trafficability (Oster and Jayawardne, 1998). Those problems are likely to be pronounced in Powder River Basin soils, such as those at the Platmak SDI site, that contain abundant swelling clays (Table 5) (Chaudhari and Somawanshi, 2004). Minimal accumulation of Na at the surface, even after six years of irrigation, gives the deep SDI system described here an advantage over surface irrigation schemes that use compositionally similar waters even following similar chemical treatments (Johnston et al., 2008, 2011). However, measureable accumulation of Na locally within some near-surface soil in SDI fields indicates that field and irrigation heterogeneities may yield problem areas over time.

Below 30 cm depth, more substantial amounts of Na added by irrigation water have accumulated in SDI soils (Fig. 5). The amount of Na in control soil between 0 and 92 cm depth can be subtracted from Na in alfalfa and grass SDI soils to obtain the amount of Na presumably accumulated due to irrigation. Those amounts are a fraction of the total Na added by irrigation water. Only 8% and 15% of total added Na has accumulated above the drip tubing in the alfalfa and grass SDI fields, respectively. The combination of low-EC and high-SAR conditions in irrigated soil between 45 and 150 cm depth could potentially impact soil structure and permeability (Figs. 4 and 5). While less problematic than if similar changes had occurred at the soil surface, such changes do have implications for soil and irrigation management. Therefore it is important to understand how such conditions develop and predict how they may evolve. The companion paper (Bern et al., 2012) documented contrasting patterns in the movement of irrigation water and solutes between soil above and below the drip tubing. The computer simulations of soil geochemistry described here illustrate how those patterns of water and solute movement translate into different pathways for the development of high sodicity and low salinity conditions in SDI soil.

Soil above the drip tubing receives irrigation water and solutes drawn upward by evaporative demand. Losses of water via evapotranspiration concentrate the solutes. Computer simulations of soil geochemistry demonstrate how increasing solute concentration by evapotranspiration drives both water (Table 5) and soil SAR values higher (Fig. 4). Comparison between the simulated and measured soil chemistry suggest solute concentration factors ranging up to ~ 13 for irrigation water (Fig. 5). Although the progression of increasing SAR values is consistent with water loss, the SAR increases do not correlate directly with increases in soil concentrations of the conservative anion Cl^- , which is also derived from irrigation water and measured in SDI soil (Bern et al., 2012). For example, maximum concentration factors calculated from extractable Cl^- are 4.5 and 26 for the alfalfa and grass SDI soils, respectively. The lack of correlation can be attributed to decoupling of the movement of Na^+ relative to Cl^- by retardation of Na^+ transport as a result of cation exchange as water moves through the SDI soil. The second transport effect influencing salinity and sodicity conditions above the drip tubing is infiltration of dilute rain and snowmelt. That infiltration lowers EC by removing ions held in soil solution, although the Na^+ on cation exchange sites maintains SAR relatively unchanged (Fig. 4). A third factor affecting soil above the drip tubing is its low gypsum content (Fig. 3). Comparison of scenario 1 and scenario 2 simulations clearly demonstrates how the lack of gypsum predisposes soil in that zone to lower EC and higher SAR (Fig. 4). In summary, upward movement of irrigation water, evapotranspiration concentration of solutes, infiltration of precipitation waters, and a lack of gypsum are responsible for high-SAR and low-EC conditions in soil above the drip tubing.

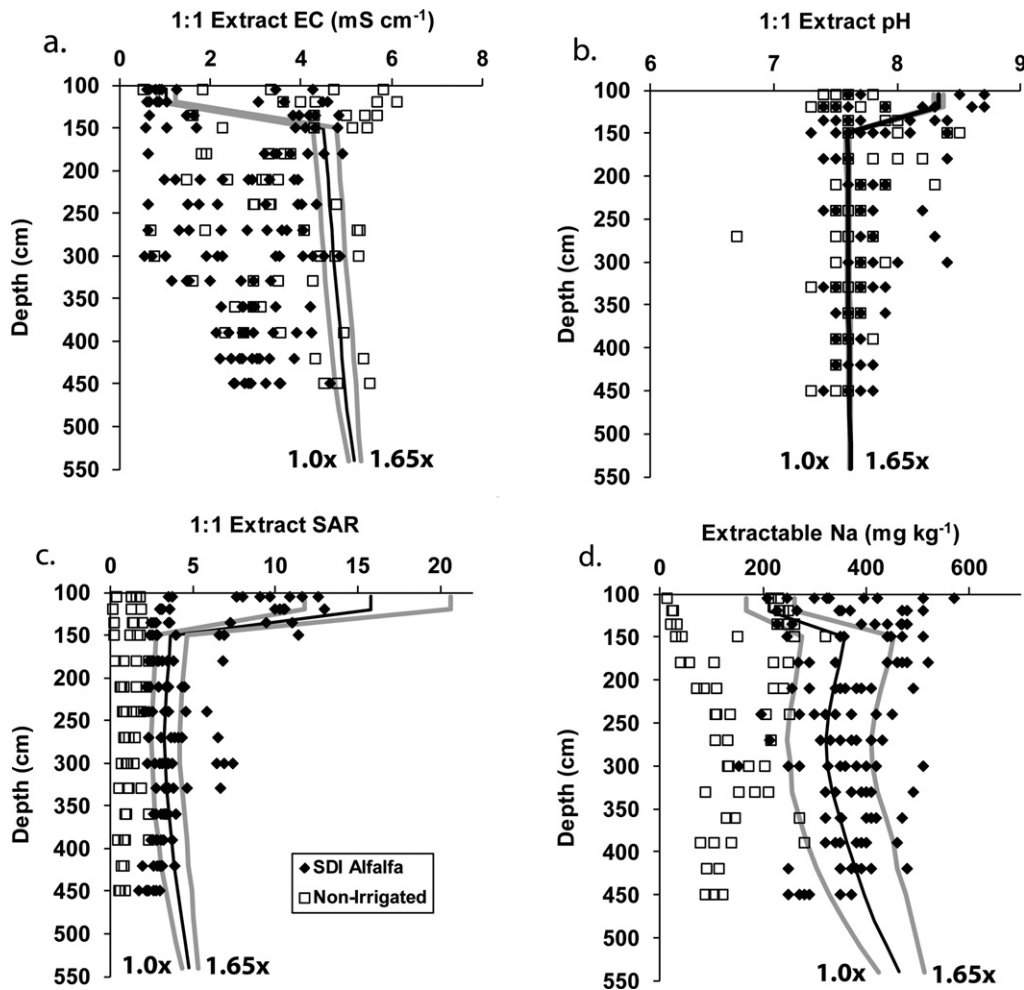


Fig. 10. Depth profiles of composition of extracts at 1:1 water–soil ratio for samples from alfalfa SDI and non-irrigated soil cores: (a) EC; (b) SAR; (c) pH; (d) extractable Na on a dry mass basis. Sample data are plotted as points versus bottom-of-sample increment depth. Output from scenario 3 of the computer simulations of soil below the drip tubing after six years of simulated irrigation are plotted as solid lines. Simulation results using a solute concentration factor of 1.3 for irrigation water are shown as a black line. Results from using factors of 1.0 and 1.65 are shown as gray lines and are labeled in the figure.

In soil beneath the drip tubing, excess irrigation water and its downward movement drive a different set of processes that also result in high-SAR low-EC conditions. One benefit of the excess irrigation water below the drip tubing is that evapotranspiration does not concentrate solutes to the levels seen above the drip tubing. Relatively low solute concentration factors ranging from 1.0 to 1.65 keep SAR from attaining higher values in soil beneath the drip tubing (Fig. 10). The high concentrations of gypsum in this zone maintain high EC and low SAR, but excess irrigation water dissolves that gypsum and percolates downward, transporting the solutes deeper in the profile. The simulations show that EC drops abruptly and SAR increases rapidly to a new steady-state value in soil where gypsum becomes depleted (Fig. 9). Continued irrigation, equilibration of irrigation water with soil, and downward transport of post-equilibration solutes therefore generate the high-SAR and low-EC conditions in soil below the drip tubing.

The simulation of irrigation with unacidified CBM water in scenario 4 illustrates the value of treatment with sulfuric acid. At the onset of irrigation, acidification has relatively little influence on SAR or EC (Fig. 7). However, by reducing precipitation of calcite, and concomitant losses of Ca^{2+} , acidification reduces the quantity of gypsum dissolved by a given quantity of irrigation water. The depletion of gypsum and onset of high-SAR, low-EC conditions that follow are therefore delayed by the sulfuric acid treatment of CBM water. After gypsum becomes depleted in a given section of soil,

acidification becomes crucial to preventing substantial changes in soil chemistry. Without acidification, SAR values rise precipitously and EC drops to relatively low values (Fig. 7). Substantial declines in soil hydraulic conductivity are anticipated as a result (McNeal and Coleman, 1966). With acidification, both SAR and EC are maintained at more moderate values, decreasing the likelihood of clay dispersion and swelling. Unacidified CBM irrigation water was also considered in a variation on simulation scenario 1 (results not shown). SAR values were elevated by 0.2–4 compared to those for scenario 1, where irrigation water was acidified. EC values were lower by as much as 1.9 mS cm^{-1} . Acidification of irrigation water is therefore crucial in limiting the development of high-SAR, low-EC conditions both above and below the drip tubing.

It is worth considering the origin and distribution of the native gypsum present at the Platmak SDI site, as it is so crucial in maintaining lower soil SAR, and higher EC. Oxidation of pyrite from local geologic sources and reaction of resulting solutions with available calcite is one possible origin. However, pedogenic gypsum in the arid Big Horn Basin 140 km to the west is identified as having an eolian source with deposition at rates of $0.01\text{--}1.2 \text{ kg m}^{-2} \text{ ky}^{-1}$ (Reheis, 1987). Gypsum at the Platmak SDI site may therefore have a similar eolian source, but the quantities present suggest longer accumulation times or greater deposition rates. More likely than either of those scenarios is that gypsum derived from both processes has been redistributed within the Powder

River Basin landscape by dissolution, transport, and precipitation interacting with local geomorphology (Schaetzl and Anderson, 2005). The Dutch Creek SDI site, 7 km away and also located on Zigweid–Kishona–Cambria complex, contains little gypsum above 100 cm depth, and up to 4% below (Bern et al., 2010) suggesting a common pattern for certain soils under the local climate. Because the gypsum is located at depth, and the threshold quantities for classification are large, these soils are not classified as gypsic and horizons sampled for taxonomic purposes generally do not qualify as gypsic (Soil Survey Staff, 2010). Therefore, while substantial gypsum may be common at depth in the Powder River Basin, soil taxonomic maps may be of limited use in locating it. Such issues should be considered when seeking sites, in the Powder River Basin or elsewhere, where SDI may benefit from native gypsum in soil.

Soil hydraulic conductivity was not measured, although the increases in soil SAR suggest potential for decreases in subsurface intervals of SDI soils (Fig. 5). Calcite precipitation, indicated in some of the simulation scenarios, could also decrease hydraulic conductivity by clogging pore spaces (Saripalli et al., 2001). Visual observations of some soil collected in SDI fields was consistent with loss of structure and clay swelling, but the high degree of water saturation made comparisons to control soils difficult. Quantification of subsurface hydraulic conductivity should be a priority for future research on the SDI system described here.

Based upon the computer simulations, and the understanding gleaned from them, predictions can be made regarding the effect of continued SDI operation by the method studied. To the extent that SDI solutes, and particularly Na^+ , become progressively concentrated in soil above the drip tubing, SAR will continue to rise. After six years of irrigation, geochemical simulations suggest solute concentration, resulting from evapotranspiration, by factors up to about 13. Without time series data it is difficult to predict the pace at which those factors might increase, driving SAR higher. The simulations make clear that infiltration of rain and snowmelt are unlikely to decrease SAR in soil above the drip tubing, and will promote conditions favorable for clay dispersion by lowering EC. Application of gypsum or a similar treatment at the soil surface, and carried downward by infiltrating precipitation, might be the most effective means of combating sodicity above the drip tubing.

Continuing to irrigate in substantial excess of crop demand will keep SAR values lower in soil below the drip tubing by keeping solute concentration factors low. Simulations extended to include fifteen years of irrigation show that both SAR and EC stabilize once gypsum is depleted in a soil zone (Fig. 9). The size of the gypsum-depleted soil zone below the drip tubing will expand progressively with continued excess irrigation. As the zone of sodic soil becomes thicker and more laterally continuous, it will pose problems for drainage of irrigation water to the extent that clay dispersion reduces hydraulic conductivity. Maintaining continuous acidification will be crucial to preventing higher SAR and lower EC conditions from developing. Treatments for soil below the drip tubing may be more costly than for soil above, as excess irrigation water will continuously remove them, necessitating continuous addition.

5. Conclusions

After six years of irrigation using acidified CBM water with an SAR value around 54, little Na has accumulated in soil between 0 and 30 cm deep in fields irrigated via deep SDI. Of the 4.6 and 3.6 kg m^{-2} of Na added to the alfalfa and grass SDI fields, only 8% and 15% have accumulated in the 0–92 cm deep interval above the drip tubing. Substantial accumulations of Na are present throughout the deeper portions of the fields. In particular, soil between 45 and 150 cm deep is becoming sodic, as indicated by high SAR. Low EC in the same soil suggests potential negative impacts on soil

structure and hydraulic conductivity. Geochemical simulations of the soil demonstrate that different processes are responsible for development of high-SAR, low-EC conditions above, versus below, the drip tubing. Above the tubing, evapotranspiration concentrates SDI solutes by factors up to 13, driving up SAR. Subsequently, infiltrating rain and snowmelt displace ions in soil solution and drive down EC. A lack of gypsum above the drip tubing also promotes development of high SAR and low EC conditions. Below the drip tubing, excess water prevents solutes from becoming as concentrated. Gypsum is present in greater quantities below the drip tubing, which maintains lower-SAR and higher-EC. Excess irrigation water progressively dissolves that gypsum and transports the resulting solutes deeper into the unsaturated zone. Sustained irrigation is expected to create zones of gypsum depletion where SAR rises and EC declines. Treatment of CBM water with sulfuric acid prior to irrigation slows the depletion of gypsum below the drip tubing. More importantly, acidification lowers SAR and raises EC in soil where gypsum is absent or has become depleted. Both the degree and spatial extent of SDI soil sodicity are likely to expand with continued irrigation using the current system. Despite that prospect, deep SDI is a viable means of deriving beneficial use from sodic waters and managing their impacts on soil.

Acknowledgements

C.R.B. was supported by a U.S. Geological Survey Mendenhall Postdoctoral Fellowship. Additional funding was provided by the USGS Energy Resources Program and the National Energy Technology Laboratory, U.S. Department of Energy. The assistance of numerous employees of BeneTerra LLC, NETL, and USGS is gratefully acknowledged. We thank Carleton and Jackie Perry for access to the Platmak study site. Mark Engle, Girisha Ganjgunte, Jim Oster, and David Parkhurst provided helpful comments on earlier versions of this paper.

Appendix A. Supplementary data

Supplementary data associated with this article can be found, in the online version, at <http://dx.doi.org/10.1016/j.agwat.2012.11.013>.

References

- Arvidson, R.S., Mackenzie, F.T., 1997. Tentative kinetic model for dolomite precipitation rate and its application to dolomite distribution. *Aquatic Geochemistry* 2, 273–298.
- Ayers, R.S., Westcot, D.W., 1985. *Water Quality for Agriculture: FAO Irrigation and Drainage Paper No. 29 (Rev. 1)*. Food and Agriculture Organization of the United Nations, Rome.
- Bajwa, M.S., Choudhary, O.P., Josan, A.S., 1992. Effect of continuous irrigation with sodic and saline-sodic waters on soil properties and crop yields under cotton–wheat rotation in northwestern India. *Agricultural Water Management* 22, 345–356.
- Bartos, T.T., Ogle, K.M., 2002. Water quality and environmental isotopic analyses of ground-water samples collected from the Wasatch and Fort Union formations in areas of coalbed methane development: implications to recharge and ground-water flow, eastern Powder River Basin, Wyoming. USGS Water-Resources Investigations Report 02-4045. 88 pp.
- Bauder, J.W., Hershberger, K.R., Browning, L.S., 2008. Soil solution and exchange complex response to repeated wetting–drying with modestly saline-sodic water. *Irrigation Science* 26, 130–212. <http://dx.doi.org/10.1007/s00271-007-0078-8>.
- Bern, C.R., Breit, G.N., Healy, R.W., Zupancic, J.W., Hammack, R., 2012. Deep subsurface drip irrigation using coal-bed sodic water: Part I. Water and solute movement. *Agricultural Water Management*, <http://dx.doi.org/10.1016/j.agwat.2012.11.014>, in press.
- Bern, C.R., Engle, M.A., Healy, R.W., Breit, G.N., Zupancic, J.W., 2010. Computer simulation of subsurface drip irrigation using coalbed methane produced waters. *Geochimica et Cosmochimica Acta* 74 (11 Suppl.), A82.
- Brinck, E., Frost, C., 2009. Evaluation of amendments used to prevent sodification of irrigated fields. *Applied Geochemistry* 24, 2113–2122.
- Brinck, E.L., Drever, J.L., Frost, C.D., 2008. The geochemical evolution of water coproduced with coalbed natural gas in the Powder River Basin, Wyoming. *Environmental Geosciences* 15 (4), 153–171.

- Burton, B.L., Bern, C.R., Minsley, B., Smith, B.D., 2010. Geophysical and Geochemical Characterization of Subsurface Drip Irrigation Sites. Fall AGU, Powder River Basin, Wyoming.
- Chaudhari, S.K., Somawanshi, R.B., 2004. Unsaturated flow of different quality irrigation waters through clay, clay loam and silt loam soils and its dependence on soil and solution parameters. *Agricultural Water Management* 64 (1), 69–90, [http://dx.doi.org/10.1016/S0378-3774\(03\)00145-8](http://dx.doi.org/10.1016/S0378-3774(03)00145-8).
- Eberl, D.D., 2003. A User's Guide to ROCKJOCK—A Program for Determining Quantitative Mineralogy from Powder X-ray Diffraction Data. USGS Open-File Report 03-78. 41 pp.
- Engle, M.A., Bern, C.R., Healy, R.W., Sams, J.I., Zupancic, J.W., Schroeder, K.T., 2011. Tracking solutes and water from subsurface drip irrigation of application of coalbed methane produced waters, Powder River Basin, Wyoming. *Environmental Geosciences*, <http://dx.doi.org/10.1306/eg.03031111004>.
- Ganjegunte, G.K., King, L.A., Vance, G.F., 2008. Cumulative soil chemistry changes from land application of saline-sodic waters. *Journal of Environmental Quality* 37, S-128–S-138, <http://dx.doi.org/10.2134/jeq2007.0424>.
- Ganjegunte, G.K., Vance, G.F., King, L.A., 2005. Soil chemical changes resulting from irrigation with water co-produced with coalbed natural gas. *Journal of Environmental Quality* 34, 2217–2227.
- Gobran, G.R., Dufey, J.E., Laudelout, H., 1982. The use of gypsum for preventing soil sodification: effect of gypsum particle size and location in the profile. *Journal of Soil Science* 33, 309–316.
- Healy, R.W., Rice, C.A., Bartos, T.T., McKinley, M.P., 2008. Infiltration from an impoundment for coal-bed natural gas, Powder River Basin, Wyoming: evolution of water and sediment chemistry. *Water Resources Research* 44 (W06424), <http://dx.doi.org/10.1029/2007WR006396>.
- Jackson, R.E., Reddy, K.J., 2007. Geochemistry of coalbed natural gas (CBNG) produced water in Powder River Basin, Wyoming: salinity and sodicity. *Water, Air, & Soil Pollution* 18, 49–61, <http://dx.doi.org/10.1007/s11270-007-9398-9>.
- Jalali, M., Merikhpour, H., Kaledhonkar, M.J., Van Der Zee, S.E.A.T.M., 2008. Effects of wastewater irrigation on soil sodicity and nutrient leaching in calcareous soils. *Agricultural Water Management* 95 (2), 143–153.
- Johnston, C.R., Vance, G.F., Ganjegunte, G.K., 2008. Irrigation with coalbed natural gas co-produced water. *Agricultural Water Management* 95, 1243–1252.
- Johnston, C.R., Vance, G.F., Ganjegunte, G.K., 2011. Soil property changes following irrigation with coalbed natural gas water: role of water treatments, soil amendments and land suitability. *Land Degradation & Development*, <http://dx.doi.org/10.1002/ldr.1132>.
- Loeppert, R.H., Hallmark, C.T., Koshy, M.M., 1984. Routine procedure for rapid determination of soil carbonates. *Soil Science Society of America Journal* 48, 1030–1033.
- Maas, E.V., Grattan, S.R., 1999. Crop yields as affected by salinity. In: Skaggs, R.W., van, Schilfgaarde, J. (Eds.), *Agricultural Drainage*. ASA-CSSA-SSSA, Madison, Wisconsin, pp.55–108.
- McNeal, B.L., Coleman, N.T., 1966. Effect of solution composition on soil hydraulic conductivity. *Soil Science Society of America Journal* 30, 308–312.
- Oster, J.D., 1982. Gypsum usage in irrigated agriculture: a review. *Fertilizer Research* 3, 73–89.
- Oster, J.D., Jayawardne, N.S., 1998. Agricultural management of sodic soils. In: Sumner, M.E., Naidu, R. (Eds.), *Sodic Soils: Distribution, Properties, Management, and Environmental Consequences*. Oxford University Press, New York, pp. 125–147.
- Parkhurst, D.L., Appelo, C.A.J., 1999. User's Guide to PHREEQC (Version 2)—A Computer Program for Speciation, Batch-reaction, One-dimensional Transport, and Inverse Geochemical Calculations. U.S. Geol. Survey Water-Resour. Inv. Rep. 99-4259. 310 pp.
- Qadir, M., Oster, J.D., 2004. Crop and irrigation management strategies for saline-sodic soils and waters aimed at environmentally sustainable agriculture. *Science of the Total Environment* 323, 1–19, <http://dx.doi.org/10.1016/j.scitotenv.2003.10.012>.
- Quirk, J.P., 1986. Soil permeability in relation to sodicity and salinity. *Philosophical Transactions of the Royal Society of London* 316, 297–317.
- Reheis, M.C., 1987. Gypsic Soils on the Kane Alluvial Fans, Big Horn County, Wyoming. U.S. Geological Survey Bulletin 1590-C. 39 pp.
- Rengasamy, P., Sumner, M.E., 1998. Processes Involved in Sodic Behavior. In: Sumner, M.E., Naidu, R. (Eds.), *Sodic Soils: Distribution, Properties, Management, and Environmental Consequences*. Oxford University Press, New York, pp. 35–50.
- Rice, C.A., Bartos, T.T., Ellis, M.S., 2002. Chemical and isotopic composition of water in the Fort Union and Wasatch formations of the Powder River Basin, Wyoming and Montana: implications for coalbed methane development. In: Schwochow, S.D., Nuccio, V.F. (Eds.), *Coalbed Methane of North America II*. The Rocky Mountain Association of Geologists, Denver, CO, pp. 53–70.
- Saripalli, K.P., Meyer, P.D., Bacon, D.H., Freedman, V.L., 2001. Changes in hydrologic properties of aquifer media due to chemical reactions: a review. *Critical Reviews in Environment Science and Technology* 31 (4), 311–349.
- Schaetzl, R.J., Anderson, S., 2005. *Soils: Genesis and Geomorphology*. Cambridge University Press, New York, NY, 832 pp.
- Suarez, D.L., Wood, J.D., Lesch, S.M., 2006. Effect of SAR on water infiltration under a sequential rain-irrigation management system. *Agricultural Water Management* 86, 150–164, <http://dx.doi.org/10.1016/j.agwat.2006.07.010>.
- Van Voast, W.A., 2003. Geochemical signature of formation waters associated with coalbed methane. *AAPG Bulletin* 87 (4), 667–676.
- Vance, G.F., King, L.A., Ganjegunte, G.K., 2008. Soil and plant responses from land application of saline-sodic waters: implications of management. *Journal of Environmental Quality* 37, S-139–S-148, <http://dx.doi.org/10.2134/jeq2007.0422>.
- Woodworth, M.T., Connor, B.F., 2003. Results of the U.S. Geological Survey's Analytical Evaluation Program for Standard Reference Samples Distributed in March 2003. USGS Open-File Report 03-281. 109 pp.
- Zupancic, J.W., Roenbaugh, J.W., Mull, G.A., Nicholson, C.M., 2008. System and method for dispersing of coal bed sodic water. Patent 7,320,559. BeneTerra, LLC (Pratt, KS). <http://patft.uspto.gov/netahtml/PTO/srchnum.htm>

Web references

- Breit, G.N. USGS Produced Waters Database: <http://energy.cr.usgs.gov/prov/prodwat/data.htm> (accessed 21.03.11).
- National Climatic Data Center. <http://www.ncdc.noaa.gov/oa/climate/stationlocator.html> (accessed 25.04.11).
- Soil Survey Staff. Soil Survey Geographic (SSURGO) Database. Natural Resources Conservation Service, United States Department of Agriculture. <http://soildatamart.nrcs.usda.gov> (accessed 7.03.11).
- Wyoming Oil and Gas Conservation Commission. <http://wogcc.state.wy.us> (accessed 21.03.11).